

Effect of generatrix profile on single-point incremental forming parameters

Mariem Dakhli¹ · Atef Boulila² · Zoubeir Tourki¹

Received: 16 January 2017 / Accepted: 31 May 2017 / Published online: 4 July 2017
© Springer-Verlag London 2017

Abstract The single-point incremental forming is one of two modes of the incremental sheet forming process. It is the most used in the manufacture of parts for small series and prototypes in various sectors such as aeronautics, bio-medical field, and art pieces. In this work, two geometries of parts are investigated at the same process parameters (rotation speed, feed rate, step increment, sheet thickness, and tool diameter). The experimental tests are made with a CNC spinner milling machine. The blank sheet of mild steel is formed by means of a hemispherical tool with a 10-mm diameter. The forming tool follows the desired spiral path that is determined by a CAD model. The main objective of this paper is to study the effects of the generatrix profile for two shapes of a truncated cone (straight and circular generatrix) on forming forces, thickness distribution, shape accuracy, and surface roughness of the formed shape. Besides, a coefficient of shape is introduced from experimental and analytical vertical forces. The experimental results show that a better roughness surface quality is obtained in forming a straight generatrix and that a more uniform thickness distribution of the blank is obtained after thinning and shaping a circular generatrix. In order to examine the geometric accuracy of the parts, a Next Engine 3D scanner is used to rebuild the developed surfaces again and to make a comparison between the programmed and scanned profiles.

Keywords Single-point incremental forming · Generatrix · 3D scanning · Thickness · Shape accuracy · Roughness

1 Introduction

The most forming process reputed for obtaining parts with complex geometries and optimizing a loss of material is the incremental sheet forming. Generally, this process, which firstly appeared in the work of Leszak in 1967 [1], is based on the plastic deformation of a thin sheet metal (less than or equal to 3 mm) using an inexpensive hemispherical tool without dies. Later, a lot of authors developed this process because of the appearance and development of the CNC machining and CAD/CAM software [2–4]. The forming tool is controlled by a CNC milling machine and it follows the path generated by the Catia software. The tool then pushes the sheet metal incrementally, which decreases the thickness of the part.

The incremental sheet forming is divided in two modes: single-point incremental forming (SPIF) and two-point incremental forming (TPIF). The main difference between these two processes is the number of contact points between the sheet and the tool. In the SPIF, the forming tool is in contact at only one point with the sheet. The blank sheet is mounted on the die and fixed by a blank holder around its edges [5]. In this paper, we involve our research in the SPIF process. However, the main drawbacks of this process are the high production time and the limit of forming the right angles [6]. On the other hand, it presents a lot of advantages such as the possibility to manufacture complex forms of sheet metal parts in a rapid and economic way without expensive dies and long setup times.

Numerous researches have been conducted to study the effect of geometries of forming tools. For that, some authors have tested the semi-spherical tool head with a radius ranged between 5 and 25 mm [7]. Moreover, others have used a

✉ Mariem Dakhli
Mariem.Dakhli@eniso.mu.tn

¹ Mechanical Laboratory of Sousse, National Engineering School of Sousse, University of Sousse, BP 264, Sousse Erriadh, Tunisia

² National Institute of Applied Science and Technology, Centre Urbain Nord, University of Carthage, BP 676 - 1080, Tunis Cedex, Tunisia

hemispherical and flat end tool to study their effects on the dimensional accuracy of the profile [8]. Some others [9–12] have examined the formability of parts manufactured by two different geometries of tools: solid hemispherical and roller ball.

The SPIF process has been carried out on different kinds of metals with various thickness, such as aluminum [13, 14], steel, brass, copper [15], titanium, magnesium and platinum alloys, thermoplastic polymers [16], and sandwich materials. These materials present the ability to deform plastically without breaking. However, many researchers have provided that some materials need greater forces to form a sheet metal such as mild steel. For instance, Ambrogio et al. [17] investigated the effect of forming force for the AA1050-O, AA3003-O, and DC04 and its relationship with formability. They showed that a tool diameter had a more significant influence on the force evolution for the list of materials investigated. Failure in materials could be caused by the increase in the wall angle. Saidi et al. [4] experimentally studied the influence of materials, the thickness, wall angle, and step-down onto the forming force. Thus, they found that the rise in one of these process parameters would raise the F_z force.

The forming forces were investigated by Duflou et al. [18] with a Kistler force (9265B). The objective was to deduce the influence of process parameters on the forces such as the step size, the tool diameter, the wall angle, and the sheet thickness. They demonstrated that the increase in one of these process parameters would ensure the growth of forces and that the augmentation at the vertical increment had a less significant effect than the other ones. Petek et al. [19] presented the experimental equipment for measuring deformations and forces in the forming of a DC05 steel metal sheet to study the influence of the wall angle, the rotation speed, the vertical increment, the tool diameter, and the lubrication on the truncated cone shape. It was illustrated that the speed rotation of the forming tool and the lubrication did not affect the forming efforts and deformations, but it had an influence on the surface quality. Furthermore, the increase in the vertical forming force is caused by the rise in one of these parameters (wall angle, tool diameter, and vertical increment).

Aerens et al. [20] defined a mathematical formula describing the three forces in function of time using different process parameters (increment, wall angle, sheet thickness, and tool diameter) for some materials such as AA3003, AA5754, DC01, AISI 304, and 65Cr2. This formula was based on the tensile strength as an input parameter to estimate the axial force F_z . Moreover, Pérez-Santiago et al. [21] had an inquiry on forming force prediction models and compared the experimental results of efforts from the literature with those calculated by the empirical equation introduced by Aerens et al. [22].

A truncated cone with circular generatrix was studied by Ziran et al. [8]. The objective of his research is to analyze the forming force for variable wall angles, from 40 to 90°, using the method reported by Duflou et al. [18].

The forming forces were analyzed by Bagudanch et al. [23] in incremental forming of a truncated cone with circular generatrix. They demonstrated that the increase in the tool diameter and axial increment would conduce to the growth of the forming force. In addition, for greater spindle speed values, the axial force would decrease.

Several authors have studied the effect of various parameters of the SPIF process and its aptitude on the surface roughness in the light of characterizing the surface quality of parts. Some authors like Junk et al. [24] have highlighted the influence of the vertical increment, the punch diameter, and the wall angle on the roughness R_z . They have done a survey of the variation in increment vertical size (0.1, 0.2, 0.5, 1 mm), tool diameters (15 and 5 mm), and wall angles (65° and 47°), and they have found that the increment has been the most factor affecting the surface finish. They have shown that the increase in the increment size induces a rise in roughness. When the forming angle and diameter are very important, the roughness will decrease. Others have noted that the surface roughness is higher in the case of non-rotating tools.

The vertical increment is the main factor responsible for determining the surface state from the formed sheets. The work performed by Jeswiet et al. [3] is investigated the role of the increment, the rotational speed on the surface state from formed parts, and roughness. By the same punch diameter (12.5 mm), these authors examined the surface state for four different values of increments. They noted that the increase in the increment size raises roughness. Lu et al. [12] studied the effectiveness of the developed oblique roller ball tool ORB and its friction effects on the formed surface formed, and they found a reduction in the coefficient of friction achieved by the ORB tool, as compared to a rigid tool. It was noted also that the ORB tool would provide a better surface finish quality. Numerous works affirmed that for a large size increment, higher roughness is offered. Thus, the size of axial and vertical increments also leads to an orange peel effect, as well. Thakur et al. [25] examined the surface roughness of a conical profile in which they varied the three following parameters such as tool diameter, step depth, and feed rate, and they presented an approach that optimize the impact of these parameters on roughness.

Gulati et al. [26] optimized the surface roughness of the formed truncated cone. They chose five factors with Taguchi's orthogonal array L18 and proved that the lubricant used in shaping had the main responsibility of reducing roughness. Hence, a better state of surface was achieved. Besides, with the use of the ANOVA test and the response table, the lubrication had a significant effect on the surface roughness, as compared to the effect of the feed rate, sheet thickness, tool radius, rotational speed, and step increment. Cerro et al. [27] determined the roughness in two directions: advancing management tool and perpendicular direction. They also showed that the roughness of AA1050-O in the perpendicular direction was greater than the one in the advancing tool direction.

Many authors like Blaga et al. [28] studied the trajectories' effects on shaping the truncated cone of a mild steel DC04 truncated cone at the same forming conditions and they deduced that the more significant trajectory would lead to obtain the best part (minimum forming forces, workpiece thickness reduction...). Others studied in their researches the geometrical accuracy of parts after the SPIF process and they made a comparison between the designed and formed profiles. Alves et al. [29] conducted an experimental investigation for formability, geometric accuracy, and surface quality of formed parts and concluded that the use of a dummy sheet between the sheet and the forming tool would permit overcoming problems of low surface quality. Else, the wall angle, the dummy sheet, and the plate thickness would affect the surface quality of formed sheets. Micari et al. [30] investigated the use of different forms of support and tool paths in the SPIF process and demonstrated that these latter can reduce the dimensional error of formed shapes in the SPIF.

Despite the importance of the works already published, the effect of a generatrix profile of formed parts has not been treated in the SPIF process yet. For that, two forms of generatrix profiles, having the same desired depth, at the same conditions are experimentally investigated. The aim of this paper is to compare the experimental results for shaping straight and circular generatrix. Moreover, we introduce a coefficient of shape in the analytical formulae describing the forming forces, which was taken from the literature. In fact, this paper deals with an experimental study of the SPIF process of two shapes: cone_T and cone_R. It is envisaged to present four responses for output parameters such as the three forming forces, roughness, sheet thickness reduction, and the shape accuracy of

manufactured parts in the same main experiment conditions. Our target is to make a comparison between the experimental results for forming two different generatrix profiles.

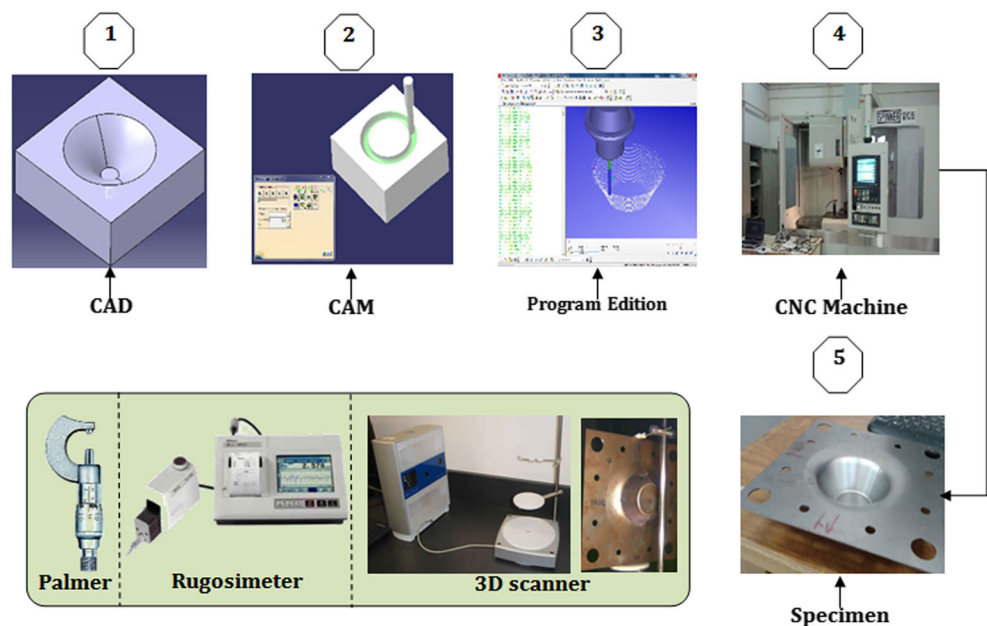
2 Experimental procedure and materials

2.1 Experimental methodology

In this work, two geometric shapes have been investigated. The most used form of steel is a mild steel with a thickness of 1 mm. This form of steel is found in the automotive industry, bridge construction, and buildings. The mild steel sheets were cut into a 200 mm × 200 mm. The experiments were accomplished on a vertical CNC machine made by Spinner MVC 850 using a steel tool diameter of 10 mm. The approach steps utilized to perform the test series of the SPIF are depicted in Fig. 1.

To conduct the previous test series of the SPIF process, we designed, first of all, two desired shapes (CAD). Then, we passed to the machining phase in which we generated the program of the forming tool path. After that, we imported the CN code in the three-axis CNC machining in case to produce the desired parts. If the incremental forming phase of the two parts is completed, three measures must be performed. Firstly, we used the 3D scanner to examine the geometric accuracy of the obtained parts. Secondly, the roughness of the inner surfaces was taken. Finally, the measure of the workpiece thickness was obtained after forming.

Fig. 1 Experimental methodology



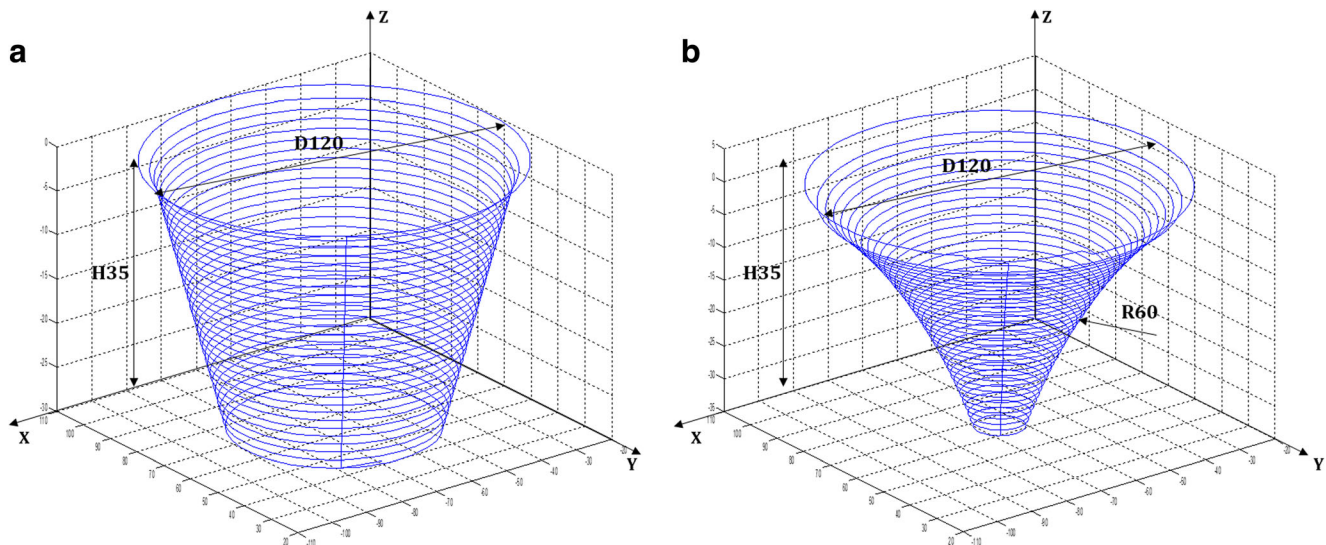


Fig. 2 Trajectories of two parts. **a** Cone_T (truncated cone with straight generatrix). **b** Cone_R (truncated cone with circular generatrix)

2.2 Specimen and trajectory

The sheets were cut by a laser process with holes in the corners to fix it in the SPIF device. It was placed on the die and fixed by a blank holder. In order to examine some response parameters like roughness and geometrical accuracy of the formed parts, we chose two generatrix types for a truncated conical shape: cone_T and cone_R which are given in Fig. 2.

2.3 Experimental apparatus

The process parameters used in a SPIF process for two truncated cones with different generatrix were 700 rpm rotation speed, 400 mm/min axial feed speed, 10 mm/min radial feed speed, and 1 mm increment. The experimental tests were accomplished on a three-axis CNC milling machine Spinner MVC850 whose specifications are given in Table 1. The experimental device was mounted on a vertical CNC milling machine containing a multi-component force sensor FN7325 with an acquisition chain used to record the forming forces, which is illustrated in Fig. 3. The force sensor was fixed onto the support plate of the SPIF device able to measure the components of efforts from 0–5 to 0–250 KN and the moments from 200 to 7000 N.m according to the three x, y, and z directions of the machine. This experimental apparatus is composed of a backing plate, a clamping plate, a sheet blank, and a forming tool. A hemispherical headed tool with a diameter of 10 mm and a length of 100 mm was chosen to deform in an incremental manner the sheet metal blank to a desired shape. In the forming material process, a friction was produced between the sheet and the tool. For that, a lubricant was utilized to reduce the friction and to get a better surface quality.

2.4 The 3D scanning

The profile definition is a crucial criteria to determine the dimensional accuracy of the employed method and to compare the programmed and obtained profile. To evaluate the spring back of the sheet material, a Next Engine 3D scanner was used. It was able to assess the efficiency of the forming process and to conduct a comparative study between the scanned profile and the initially programmed one.

This scanner is based on the optical acquisition of surfaces. The geometric accuracy of this 3D scanner is around ± 0.005 mm. Firstly, it is necessary to fix the object to scan on the turntable which is driven by the scanner. It is clamped between bottom clamp and top clamp. If the scanned surface is transparent, it is necessary to spray on a reflective powder. After that, the scan parameters will be defined, namely positioning, target, and range. Furthermore, it is indispensable to choose the number of steps for the test piece to turn a full tour and sweep all surfaces of the sheet and to specify as well the time accuracy and the distance between the object and the scanner.

This process occurs in three stages. In the first stage, an optical acquisition of the developed surfaces is ensured. Then, a conversion of the captured images during the scan is translated via the Scan Studio software. When the scan campaign ends, the assembly of these scans will be the next step that will

Table 1 The specification of used machine

Axis number	3	
Axis travel	Longitudinal travel X	850 mm
	Transversal travel Y	510 mm
	Vertical travel Z	510 mm
Spindle speed	6000 rpm	

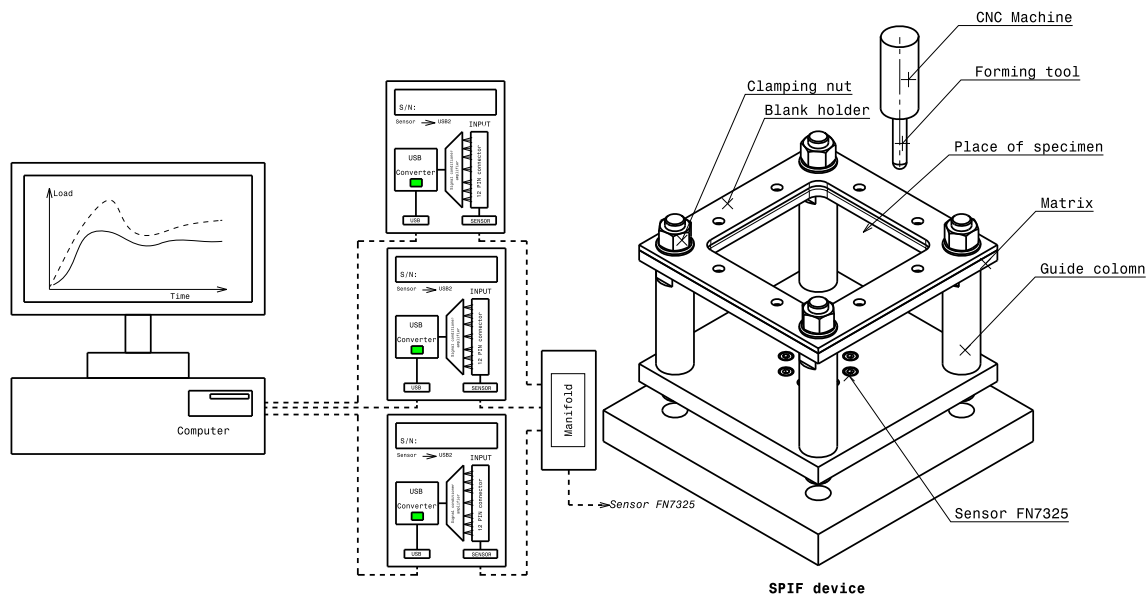


Fig. 3 Experimental device used for SPIF process

need more time. Afterwards, it should be cleaned of any soft space element (delete, merge, polish). Once the cleaning of the model is completed, it is time to smooth the model. Figure 4 details the steps followed for digitalizing the shape. After that, we import this file into the Catia software and generate the CAD model.

3 Results and discussions

In this section, we are interested in the experimental results of the SPIF process, while analyzing the effect of the two generatrix shapes on the radial and axial forces, the workpiece thickness, the shape accuracy, and the roughness.

3.1 Forming force

The forming forces are obtained using a multi-component force sensor in three directions, OX, OY, and OZ, where the OZ direction corresponds to the Z-axis of the CNC machine. Since the values of F_x and F_y forces are almost equal with a phase shift, we consider the radial force F_r that represents F_x and F_y .

It is demonstrated that the vertical forming force reaches a maximum value equal to 1830 N at 500 s for the circular generatrix shape (cone_R), as can be seen in Fig. 5. For the straight generatrix (cone_T), the maximum vertical forming force can reach 1500 N with a difference of 18%. This difference can be explained by the effect of the circular generatrix that needs a greater force to deform the sheet metal in the same experiment conditions. A small difference is observed between the radial forces and it has a phase shift of $(\pi/2)$. Thus, the maximum value

of the vertical load is four times as equal as the maximum value of radial one for the circular generatrix cone and almost three times for the straight generatrix one.

There is no significant difference between the two shapes during the first 200 s. For the radial force, $F_r = f(t)$ constitutes a sinusoidal envelope. The radial forces are evolving periodically. Initially, the radial force is beginning to increase in the range of [200,500] seconds. Therefore, every peaks of each increment defines a vertical line. Then, it is stabilized until the end of forming. After pushing the material down to 1 mm, the tool conducts an outline in which it sweeps the surface of the metal sheet that is in contact with the tip of the tool. Thus, in each outline, the radial forces are reaching a maximum and a minimum that are equal in an absolute value. The difference in terms of vertical loads from both geometries is explained by a need for a greater amount of strain energy in order to get the circular generatrix by deforming the sheet metal. We can divide the evolution of the vertical forces (axial forces) generated by the SPIF to cone_T and cone_R in two stages, where the axial force during the first phase is an increasing function, whereas within the second stage, it tends to be steady.

In reviewing the experimental results of efforts, we can deduce from varying geometries of the desired generatrix at the same process that there is a difference of 300 N in vertical forces, which can be explained by the concavity of the generatrix. For this, we need more energy to deform the sheet metal.

Some authors have studied the evolution of the vertical forces and have predicted them by an analytical equation that combines the experiment process parameters.

Fig. 4 Steps followed for digitalization of surfaces. **a** Scan attachment device. **b** Cleaning. **c** Assembly of the scans. **d** Smoothing and optimizing model

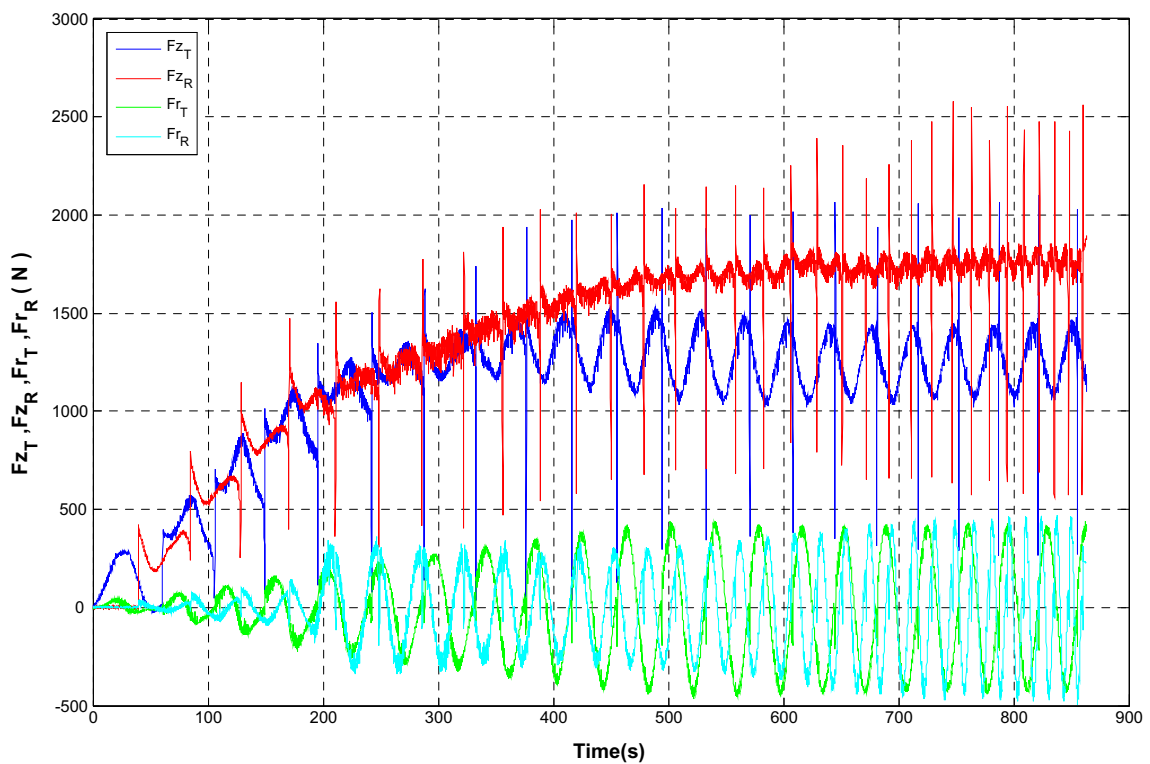
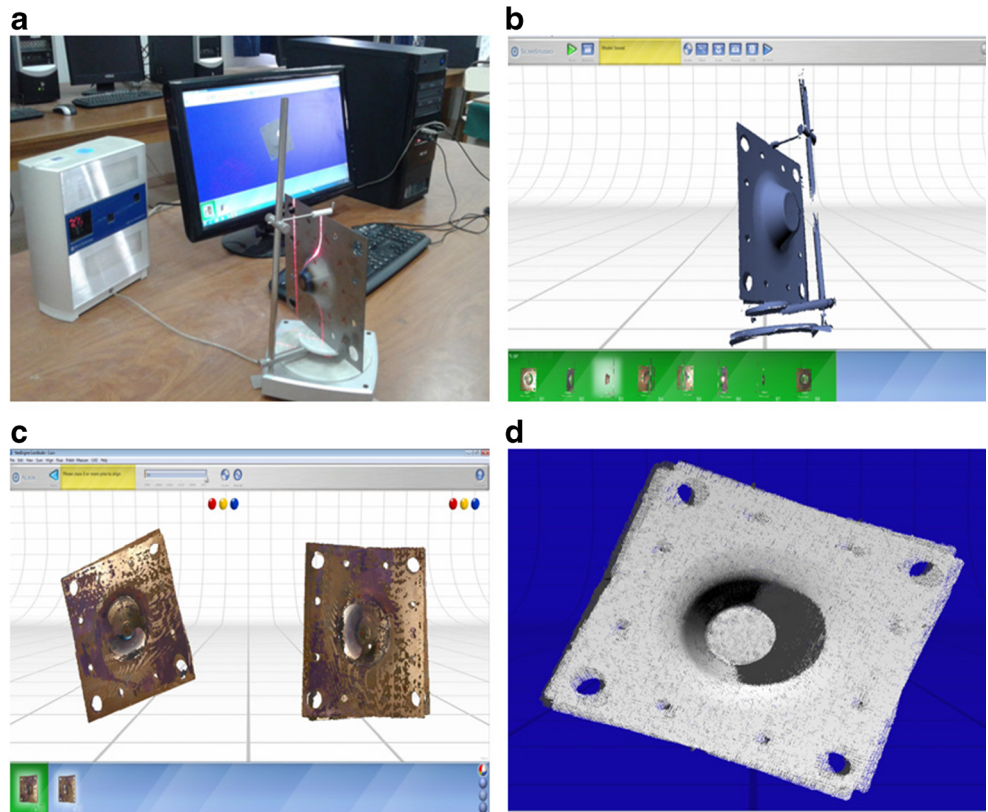


Fig. 5 Results of forming forces of two formed parts (F_{r_R} and F_{z_R} for cone_R, F_{r_T} and F_{z_T} for cone_T)

Table 2 Comparison between analytical and experimental vertical load for cone_T and cone_R

	Point	h (mm)	α (°)	Δh	Fz_s any	Fz_{exp}	Error (%)	Coefficient of shape
Cone_T	A	0	60	0.03333	853.71	1250	31.7	$K_T = 0.68$
Cone_R	A	0	25.94	0.130654	750.64	1350	44.39	$K_R = 0.55$
	a	8.75	37.94	0.066461	904.76	1630	44.49	$K_R = 0.55$
	b	17.5	43.12	0.053509	934.64	1750	46.59	$K_R = 0.53$
	c	26.25	55.17	0.037103	905.37	1751	48.29	$K_R = 0.51$

Equation (1) was used by Aereus et al. [20] after determining the scallop height:

$$Fz_s = 0.0716R_m t^{1.57} d_t^{0.41} \Delta h^{0.09} \alpha \cos(\alpha) \tag{1}$$

$$\Delta h = \left(\frac{\Delta z}{4 \sin^2 \alpha d_t} \right)^2$$

The working-condition parameters of prediction loads are classified in Table 2. For both cone forms, we calculate the vertical forces at points A, a, b and c, as indicated in Fig. 6, for each wall angle. The used process parameters are R_m for the tensile strength of material, t for the thickness of the blank sheet, d_t for the diameter of the tool, Δz for the scallop height, and α for the wall angle.

On the other hand, we compared the experimental results to the analytical ones. Petek et al. [19] used the same parameters in the incremental forming process of a truncated cone whose used material was mild steel DC05, thickness was 1 mm, and tool diameter was 10mm. Analytically, the predicted vertical force by Eq. (1) is equal to 1732.20 N. We compared this value to the experimental vertical force obtained in the work of Petek. An error of 7% was found, which was the first interpretation in agreement with the experimental results for forming cone_T.

Table 3 summarizes the data process utilized to predict the forming forces by the analytical Eq. (1) in forming a truncated cone with constant (cone_T) and a variable wall angle (cone_R). The analytical predictions were compared to the experimental force for aluminum alloys such as 7000 and 3000 series. Based on these predictions of aluminum sheet metals, we compared the effort in forming a mild steel sheet metal of cone_R and we found that these predictions did not follow the experimental ones in the last wall angle.

To comply with Eq. (1), we define Eq. (2) that introduces a coefficient of the shape K_i , $i = T$ or R for (cone_T) or (cone_R), to check for other forms:

$$Fz_s \text{ any} = K_i \cdot Fz_{exp} \tag{2}$$

The coefficient of shape is a constant that depends on the form of the generatrix. In this present work, the calculated coefficient of shape is variable from one model to another, which can be seen in Table 2. The K_T is equal to 0.68. For cone_R, the K_R varies from 0.51 to 0.55. As presented in Table 3, we calculate the coefficient of shape for other studies in cone_T and cone_R. We find a difference of 18 and 6%, respectively for cone_T and cone_R, in the coefficient of shape between the literature and our work. This difference can be explained by the stiffness of the used tip tool (tool material), the feed rate, and the rotation speeds as well as the lubricant used during incremental forming. Regarding the pyramidal shape from the literature, K_p is equal to 0.8. Equation (2) may be applicable for these works [10, 31, 32]. Therefore, the analytical values of forming forces can be determined.

3.2 Workpiece thickness

In order to analyze the thickness reduction in both geometries, the parts deformed by the forming process were cut in the median plane through the x -axis or the y -axis. This method could cause damage at the surface of the sheet metal. Then, the

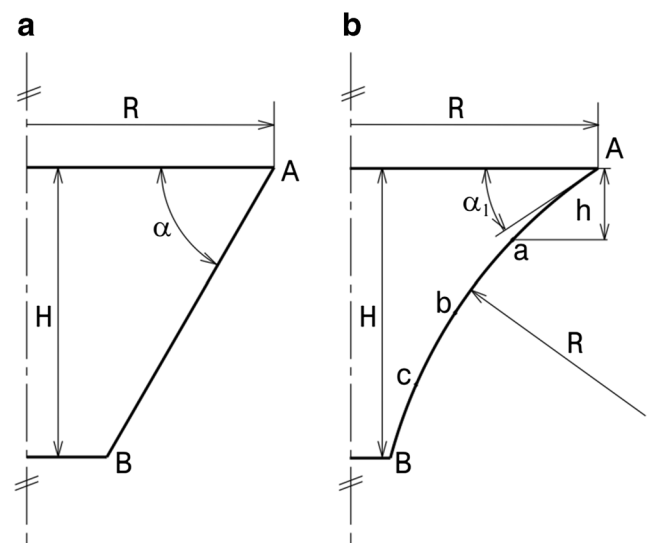


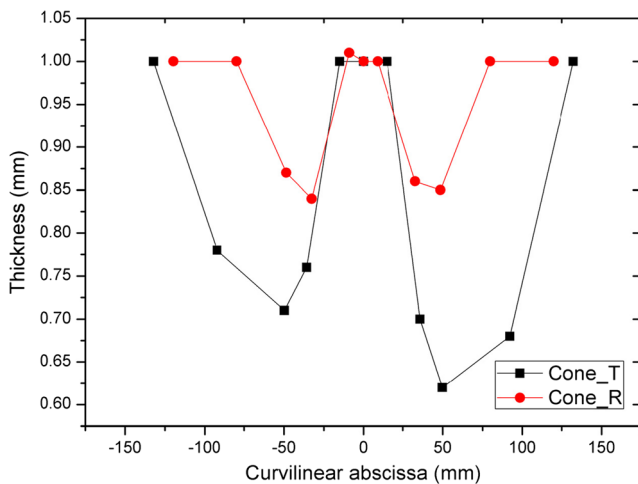
Fig. 6 Constant wall angle and variable wall angle at indicated points. **a** Straight generatrix. **b** Curved generatrix

Table 3 Analytical and experimental vertical load for different aluminum alloy material: cone_T and cone_R

Authors	Shape	Material	t	Δz	α (°)	Δh	$Fz_{s\text{ anly}}$	Fz_{exp}	Error (%)	Coefficient of shape
Duflou, 2007	Cone_T	AA3003-O	1.2	0.5	50	0.01065	601.76	550	9.41	$K_T = 0.83$
Bouffioux, 2010	Cone_T	AlMgSc	0.5	0.5	40	0.01513	458.49	460	-0.33	$K_T = 0.99$
Eyckens, 2010	Cone_T	AA3003-O	1.2	0.744	60	0.01845	564.53	520	8.56	$K_T = 0.92$
Ziran, 2010	Cone_R	AA3003-O	1	0.5	40	0.015127	390.23	300	30.08	$K_R = 0.76$
					50	0.010651	396.58	300	32.19	$K_R = 0.75$
					60	0.008333	362.10	300	20.70	$K_R = 0.82$
					70	0.007078	284.76	300	-5.08	$K_R = 0.94$
					80	0.006444	163.84	300	-45.39	$K_R = 0.54$

thickness was measured by means of a micrometer throughout the x -axis all along the inner profile of the sheet in both cases.

Based on the curves shown in Fig. 7, the thickness variation in the undeformed regions remains almost constant. A slight variation in these areas is reflected by spring back of material. In the affected areas by the forming tool, the thickness reduction is very important as regards cone_T. It varies from 1 to 0.62 mm. However, the thickness reduction of cone_R does not exceed 0.8 mm. Through the action of the

**Fig. 7** Thickness distribution with curvilinear abscissa for two geometries**Fig. 8** Depth measured by trusquin

tool tip on the metal sheet, a local heating is produced within the pressure areas.

For forming generatrix profiles, the material of the sheet is prepared to draw the wall angle in the first outlines of the path. Furthermore, for cone_R, the forming angle in the first outlines (around 26°) is lower than the forming angle for cone_T (equal to 60). A greater variation in reduction thickness between these two generatrix is explained by the forming angle. The rise in the wall angle through a circular generatrix leads to a minimum thickness reduction (closer to the initial value of the sheet before forming).

3.3 Shape accuracy

In terms of determining which of the two generatrix is more accurate, the scanner 3D was used. We reconstructed the scanned surfaces of cones by starting from cloud of points using a quick surface reconstruction workshop to finally get the deformed profile. A comparison has been made between the desired and scanned profiles. Thus, we measured the depth reached by the trusquin (Fig. 8).

As it can be noticed in Figs. 8 and 9, the comparison between the scanned and the programmed profile is made. The designed depth of cone_R is not attained because the circular radius has exceeded the programmed radius. The scanned depth and radius are respectively equal to 32.56 and 69.63 mm. There is an

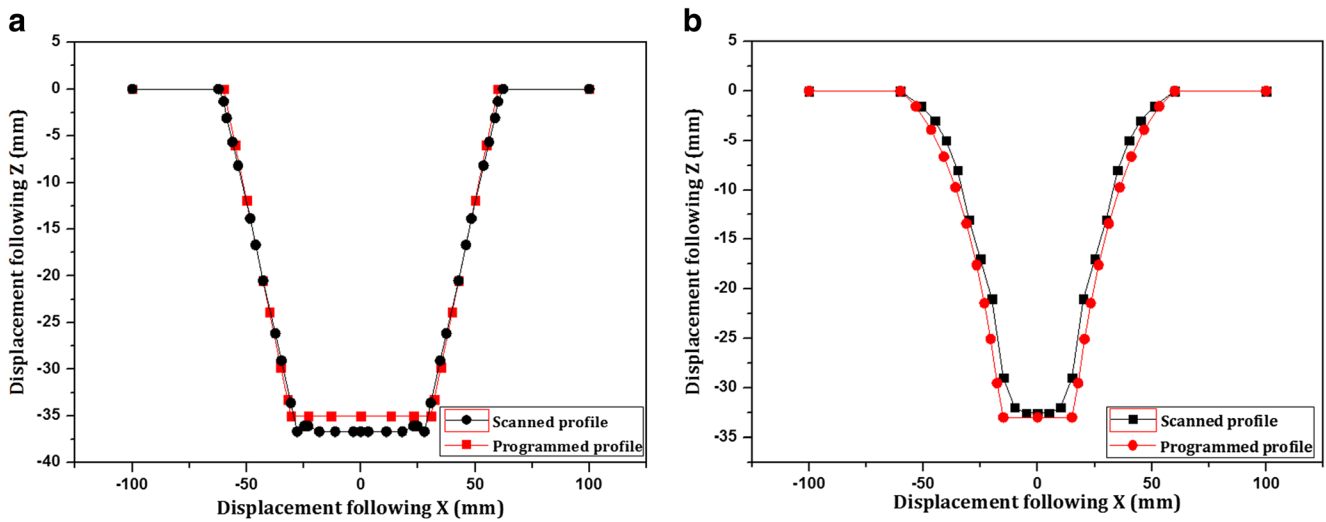


Fig. 9 Comparison between programmed and scanned profiles in the two truncated cones. a Cone_T. b Cone_R

error of 7% in the depth and 16% in the radius between the obtained and programmed geometric parameters. This gap is caused by the curvature of convexity and the behavior of the material. Concerning cone_T, the value of the obtained height has overestimated the programmed one. There is an error of 4.8% between the measured depth by a trusquin and the programmed one.

3.4 Roughness

The analysis of micro-geometrical defects of machined surfaces was performed by measuring roughness with a

rugosimeter. The most studied and exploited parameters in predicting the quality of the finished surface texture parameters have been Rz for the maximum height profile and Ra for the arithmetic mean deviation of the profile. The roughness measurements were taken on the inner portion of the shape of the workpiece all along the *x*- and *y*-axes in the three zones represented in Fig. 10.

The roughness tester has to collect data throughout the distance traveled by the feeler. The evaluation distance in the three zones is 4 mm. Figure 11 depicts an example of a profile measured through zone1 in the direction of the *x*-axis. These taken measurements were compared with the value of

Fig. 10 Zones of roughness measurements

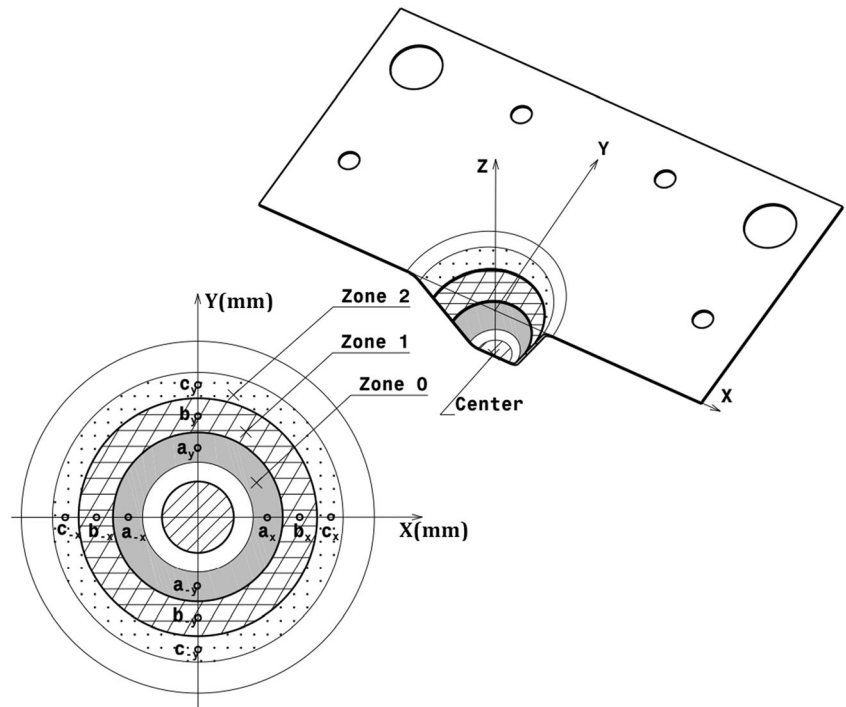


Fig. 11 Roughness profile measured in zone1 at b_x



roughness in the undistorted area. The comparisons between the measures of the two obtained specimens were used to determine which of two parts would offer a better surface finish.

The histogram presented in Fig. 12 is exploited to compare the relationship that exists between the geometry of the manufactured parts and the roughness. The values of the roughness correspond to the average of the roughness measured at the points a, b, and c of the corresponding zones. The initial roughness R_a for cone_T and cone_R is respectively 1.68 and 4.1 μm .

The arithmetical mean roughness profile in case of cone_R is higher than the roughness in case of cone_T. Added to that, the percentage of the maximum and minimum arithmetic mean profile deviations was calculated with respect to the initial roughness of the workpiece before forming. In fact, a significant increase in percentage from the arithmetic mean roughness from 11.3 to 51% was found in relation to the truncated shape with a straight generatrix, contrary to a slight increase for cone_R.

The results analyzed in Fig. 12a demonstrate that a better and lower roughness surface is obtained in forming a complex generatrix profile that has mere generatrix without a variant wall angle. Moreover, the

roughness surfaces along zone0, zone1, and zone2 are mentioned. From the earliest outlines, there is a very significant increase in the mean roughness depth at the first contact between the tool and the sheet metal, compared to the roughness in the borders of the sheet. The arithmetic mean deviation of the profile is almost constant throughout the various contours. Thus, R_a varies gradually from zone2 to zone0 for cone_T. It goes up in the first outlines (zone2), then goes down. After that and, in the last outlines (zone0), R_a stabilizes. On the side of cone_R, the variation in terms of surface roughness is important. The same tendency was observed in previous studies [33–35].

4 Conclusions

Two parts with different geometries of generatrix have been investigated at the same process parameters. These latter are tool diameter, rotation speed, feed rate, step increment, and sheet thickness. An optimum tool diameter and lubrication have been used to achieve a better geometrical accuracy and to get a better surface quality. Under the light of this study, there are some relevant results:

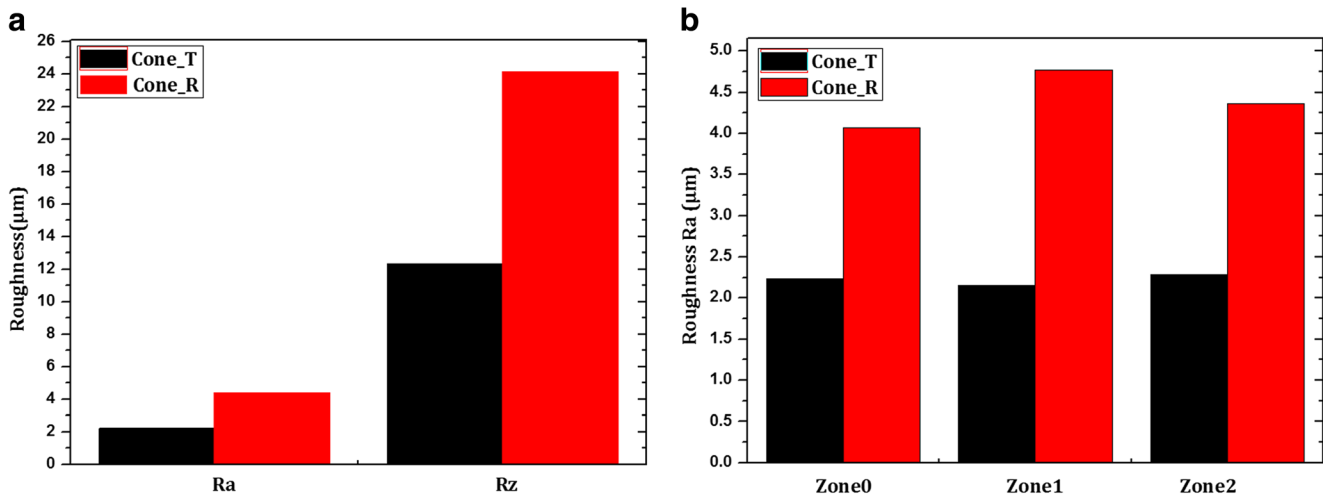


Fig. 12 Experimental roughness surface corresponding to cone_T and cone_R. **a** R_a and R_z . **b** R_a along three zones

- A concordance between the analytical and experimental forming force values for cone_T has been achieved.
- For the mild steel material and for shaping cone_R, there has been a large difference between the analytical and experimental forces.
- The model prediction of the forming forces was offered by Aerens et al. It did not take into account the other geometric parameters such as the programmed depth and the profile generatrix that determined the desired form. It used one single geometric parameter that described the shape (the wall angle) at the side of the sheet thickness, the tool diameter, the material of the sheet, and the increment. Through this paper, we have shown the utility of the corrective factor, called coefficient of shape.
- In this study, the K_T and K_R shapes varied between 0.5 and 0.9, so Eq. 2 is not applicable. This will be the subject of our future work.
- We can determine the analytic forming force in the case of a pyramidal form with a coefficient of shape ($K_p=0.8$).
- There is a significant difference in thickness, around 26%, in deformed regions between both geometries (cone_T and cone_R).
- A circular generatrix with a step-by-step increase in the forming angle can perform a minimum thickness reduction (around 0.8 mm), compared to the straight generatrix (0.6 mm).
- Forming a complex generatrix has led to a better thickness distribution. However, the stretch of the material has not reached the programmed depth.
- In favor of determining the best formed generatrix in constant process parameters, the geometrical accuracy of the generatrix profiles has been studied by measuring the error between the formed and designed heights. In addition, the gap between the obtained and designed profiles has been determined by reconstructing the formed surfaces. This deviation is explained by the material behavior and the geometry complexity.
- All along the tool path, the surface roughness Ra of cone_R is very significant. With the increase in the wall angle for forming a concave generatrix, the roughness surface goes up and then goes down.

Compliance with ethical standards

Conflict of interest The authors declare that they have no conflict of interest.

References

1. Leszak E (1967) Apparatus and process for incremental dieless forming. United States Patent Office US3342051
2. Matsubara S (2001) A computer numerically controlled dieless incremental forming of a sheet metal. *Proc Inst Mech Eng Part BJ Eng Manuf* 215:959–966
3. Jeswiet J, Micari F, Hirt G, Bramley A, Dufloy J, Allwood J (2005) Asymmetric single point incremental forming of sheet metal. *CIRP Ann Manuf Technol* 54(2):88–114
4. Saidi B, Boulila A, Ayadi M, Nasri R (2015) Experimental force measurements in single point incremental sheet forming SPIF. *Mech Ind*. doi:10.1051/meca/2015018
5. Benmessaoud R (2014) A tool path generation method for the multi-pass incremental forming process investigation. *Int J Adv Res Comp Sci Softw Eng* 4(5):1035–1044
6. Nicolas D (2009) Formage incrémental de tole d'aluminium: étude du procédé à l'aide de la mesure de champs et identification de modèles de comportement. Ph.D. thesis, Toulouse-III-Paul-Sabatier University, France
7. McAnulty T, Jeswiet J, Doolan M (2017) Formability in single point incremental forming: a comparative analysis of the state of the art. *CIRP J Manuf Sci Technol* 16:43–54
8. Xu Z, Gao L, Hussain G, Cui Z (2010) The performance of flat end and hemispherical end tools in single-point incremental forming. *Int J Adv Manuf Technol* 46(9):1113–1118
9. Kim YH, Park JJ (2002) Effect of process parameters on formability in incremental forming of sheet metal. *J Mater Process Technol* 130:42–46
10. Durante M, Formisano A, Langella A (2011) Observations on the influence of tool-sheet contact conditions on an incremental forming process. *J Mater Eng Perform* 20(6):941–946
11. Li Y, Liu Z, Daniel WJT, Meehan PA (2014) Simulation and experimental observations of effect of different contact interfaces on the incremental sheet forming process. *Mater Manuf Process* 29:121–128
12. Lu B, Fang Y, Xu DK, Chen J, Ou H, Moser NH, Cao J (2014) Mechanism investigation of friction-related effects in single point incremental forming using a developed oblique roller-ball tool. *Int J Mach Tools Manuf* 85:14–29
13. Hussain G, Khan HR, Gao L, Hayat N (2013) Guidelines for tool-size selection for single-point incremental forming of an aerospace alloy. *Mater Manuf Process* 28:324–329
14. Fang Y, Lu B, Chen J, Xu DK, Ou H (2014) Analytical and experimental investigations on deformation mechanism and fracture behavior in single point incremental forming. *J Mater Process Technol* 214:1503–1515
15. Thibaud S, Ben Hmida R, Richard F, Malécot P (2012) A fully parametric toolbox for the simulation of single point incremental sheet forming process: numerical feasibility and experimental validation. *Simul Model Pract Th* 29:32–43
16. Bagudanch I, Garcia-Romeu ML, Sabater M (2016) Incremental forming of polymers: process parameters selection from the perspective of electric energy consumption and cost. *J Clean Prod* 112:1013–1024
17. Ambrogio G, Dufloy J, Filice L, Aerens R (2007) Some considerations on force trends in incremental forming of different materials. 10th ESAFORM Conference on material forming ([HYPERLINK "http://AIP.Scitation.Org/journal/apc"](http://AIP.Scitation.Org/journal/apc) AIP Conference proceedings), American Institute of Physics
18. Dufloy J, Tunçkol Y, Szekeres A, Vanherck P (2007) Experimental study on force measurements for single point incremental forming. *J Mater Process Technol* 189(1–3):65–72
19. Petek A, Kuzman K, Kopaè J (2009) Deformations and forces analysis of single point incremental sheet metal forming. *Arch Mater Sci Eng* 35:107–116
20. Aerens R, Eyckens P, Van Bael A, Dufloy JR (2010) Force prediction for single point incremental forming deduced from experimental and FEM observations. *Inter J Adv Manuf Technol* 46:969–982

21. Pérez-Santiago R, Bagudanch I, García-Romeu ML (2011) Force modeling in single point incremental forming of variable wall angle components. *Key Eng Mater* 473:833–840
22. Aerens R, Duflou JR, Eyckens P, Van Bael A (2009) *Inter J Mater Form* 2:25–28
23. Bagudanch I, Centeno G, Vallellano C, Garcia-Romeu ML (2013) Forming force in Single Point Incremental Forming under different bending conditions. *MESIC The Manufacturing Engineering Society International Conference*. Elsevier Ltdp. 354–360
24. Junk S, Hirt G, Bambach M, Chouvalova I, Ames J. (2003). Flexible CNC flexible CNC incremental sheet forming: process evaluation and simulation. *Conferência Nacional de Conformação de Chapas, 15, Outubro Porto Alegre/RS, Brasil*, ed. Schaeffer L, Gráfica e Editora Brasul Ltda p. 30-38.
25. Thakur R, Kumar N (2015) Optimization of surface roughness and improving profile accuracy in SPIF (single point incremental forming) process. *Inter J Curr Eng Technol* 5:2048–2052
26. Gulati V, Aryal A, Katyayal P, Goswami A (2016) Process parameters optimization in single point incremental forming. *J Inst Eng India Ser C* 97:185–193
27. Cerro I, Maidagan E, Arana J, Rivero A, Rodríguez PP (2006) Theoretical and experimental analysis of the dieless incremental sheet forming process. *J Mater Process Technol* 177(1–3):404–408
28. Blaga A, Oleksik V (2013) A study on the influence of the forming strategy on the main strains, thickness reduction, and forces in a single point incremental forming process. *Adv Mater Sci Eng*. doi: [10.1155/2013/382635](https://doi.org/10.1155/2013/382635)
29. Alves ML, Silva MB, Alves LM, Martins PAF (2009) On the formability, geometrical accuracy and surface quality of sheet metal parts produced by SPIF. *Proc. SPIE 7375ICEM 2008: International Conference on Experimental Mechanics*
30. Micari F, Ambrogio G, Filice L (2007) Shape and dimensional accuracy in single point incremental forming: state of the art and future trends. *J Mater Process Technol* 191:390–395
31. Durante M, Formisano A, Langella A, Capece Minutolo FM (2009) The influence of tool rotation on an incremental forming process. *J Mater Process Technol* 209(9):4621–4626
32. Rauch M, Hascoet JY, Hamann JC, Plenel Y (2009) Tool path programming optimization for incremental sheet forming applications. *Comput Aided Design* 41:877–885
33. Cavalier LCC, Schaeffer L, Rocha AS, PERUCH F (2010) Surface roughness in the incremental forming of AISI 304L stainless steel sheets. *Far East J Mech Eng Phys* 1:87–98
34. Arshad S (2012) A study of forming parameters, forming limits and part accuracy of aluminium 2024, 6061 and 7475 alloys. PhD. thesis, KTH Royal Institute of technology Stockholm, Sweden
35. Gatea S, Ou H, McCartney G (2016) Review on the influence of process parameters in incremental sheet forming. *Int J Adv Manuf Technol* 87:479–499